J|A|C|S
ARTICLES
Published on Web 03/19/2002

Rate-Equilibrium Relationships in Hydride Transfer Reactions: The Role of Intrinsic Barriers

Ernst-Ulrich Würthwein,*,† Gabriele Lang,‡,§ Ludwig H. Schappele,‡,|| and Herbert Mayr*,‡

Contribution from the Institut für Organische Chemie der Westfälischen Wilhelms-Universität Münster, Corrensstrasse 40, D-48149 Münster, Germany, and Department Chemie der Ludwig-Maximilians-Universität München, Butenandtstrasse 5-13 (Haus F), D-81377 München, Germany

Received September 10, 2001

Abstract: A literature survey on the kinetics of hydride abstractions from CH-groups by carbocations reveals a general phenomenon: Variation of the hydride acceptor affects the rates of hydride transfer to a considerably greater extent than an equal change of the thermodynamic driving force caused by variation of the hydride donor. The origin of this relationship was investigated by quantum chemical calculations on various levels of ab initio and DFT theory for the transfer of an allylic hydrogen from 1-mono- and 1,1-disubstituted propenes ($XYC{=}CH{-}CH_3$) to the 3-position of 1-mono- and 1,1-disubstituted allyl cations ($XYC{=}CH{-}CH_2^+$). The discussion is based on the results of the MP2/6-31+G(d,p)//RHF/6-31+G(d,p) calculations. Electron-releasing substituents X and Y in the hydride donors increase the exothermicity of the reaction, while electron-releasing substituents in the hydride acceptors decrease exothermicity. In line with Hammond's postulate, increasing exothermicity shifts the transition states on the reaction coordinate toward reactants, as revealed by the geometry parameters and the charge distribution in the activated complexes. Independent of the location of the transition state on the reaction coordinate, a value of 0.72 is found for Hammond−Leffler's $\alpha = \delta\Delta G^{\ddagger}/\delta\Delta_r G^{\circ}$ when the hydride acceptor is varied, while $\alpha = 0.28$ when the hydride donor is varied. The value of α thus cannot be related with the position of the transition state. Investigation of the degenerate reactions $XYC{=}CH{-}CH_3 + XYC{=}CH{-}CH_2^+$ indicates that the migrating hydrogen carries a partial positive charge in the transition state and that the intrinsic barriers increase with increasing electron-releasing abilities of X and Y. Substituent variation in the donor thus influences reaction enthalpy and intrinsic barriers in the opposite sense, while substituent variation in the acceptor affects both terms in the same sense, in accord with the experimental findings. Marcus theory is employed to treat these effects quantitatively.

Introduction

It has long been known that there is a general correspondence between rates and heats of chemical reactions. Within a series of related reactions, very exothermic reactions usually take place faster than less exothermic ones. Numerous quantitative treatments of such relationships have been reported (eq 1),[1,2] and Dewar suggested referring to them collectively as the Bell−Evans−Polanyi principle.[3]

$$\Delta E^{\ddagger} = A + B\Delta H \qquad (1)$$

One of the consequences of the Bell−Evans−Polanyi principle is the well-known Hammond postulate[4] and the Hammond−Leffler relationship[1] (eq 2), which provides a quantitative correlation between structural effects on rates and equilibria of chemical reactions.

$$\delta\Delta G^{\ddagger} = \alpha\delta\Delta G^{\circ} \qquad (2)$$

$\delta\Delta G^{\circ}$ expresses the change of the reaction free energy, induced by structural variation, and the proportionality constant α reflects the fraction of this effect that is observable in the activation free energy $\Delta G^{\ddagger}$. The magnitude of α has often been used for localizing transition states, but it is well-known that the assumption $0 < \alpha < 1$ and the association of small values of α with early transition states, and of large values of α with late transition states, is too simplistic.[5] Such relationships have extensively been investigated in proton-transfer reactions. Changes of ΔG° due to variation of the base have been found

* To whom correspondence should be addressed. E.-U.W.: Fax (internat.), +49(0)251/83-39772; E-mail, wurthwe@uni-muenster.de. H.M.: Fax (internat.), +49(0)89/2180-7719; E-mail, Herbert.Mayr@cup.uni-muenchen.de.
† Westfälische Wilhelms-Universität Münster.
‡ Ludwig-Maximilians-Universität München.
§ Current address: BASF AG, Polymer Laboratory, D-67056 Ludwigshafen, Germany.
|| Current address: Ems-Dottikon AG, CH-5605 Dottikon, Switzerland.

(1) Leffler, J. E.; Grunwald, E. *Rates and Equilibria of Organic Reactions*; Wiley: New York, 1963.
(2) Chapman, N. B.; Shorter, J. *Advances in Linear Free Energy Relationships*; Plenum Press: London, 1972.
(3) Dewar, M. J. S.; Dougherty, R. C. *The PMO Theory of Organic Chemistry*; Plenum Press: New York, 1975.
(4) Hammond, G. S. *J. Am. Chem. Soc.* **1955**, *77*, 334−338.

10.1021/ja0121540 CCC: $22.00

Table 1. Calculated (AM1) and Experimental Hydride Affinities (kcal mol^{-1}) of Some Conjugated Carbenium Ions Derived from the Corresponding Heats of Formation

	AM1			gas-phase data		
R–H	$\Delta_f H°$(R–H)	$\Delta_f H°$(R$^+$)	HIA[a]	$\Delta_f H°$(R–H)	$\Delta_f H°$(R$^+$)	HIA[b]
cycloheptatriene (**1a**)	38.2	210.4	257.8	44.6[c]	208.9[d]	199.0
1,4-cyclohexadiene (**1b**)	16.9	205.9	274.6	25.0[c]	207.1[e]	216.8
1,4-dihydronaphthalene (**1c**)	27.4	213.0	271.2	33[f]	210.5[e]	212
9,10-dihydroanthracene (**1d**)	38.4	221.1	268.3	38.2[g]	213.1[e]	209.6
xanthene (**1e**)	18.2	198.1	265.5			
4-methyl-2,5-heptadiene (**1f**)	2.5	181.9	265.0			
2,5-heptadiene (**1g**)	4.8	190.9	271.7			
3-methyl-1,4-pentadiene (**1h**)	20.6	211.8	276.8			
1,4-pentadiene (**1i**)	24.6	222.5	283.5	25.2[g]	(220.4)[d]	229.9
3-propylcyclopentene (**1j**)	−15.2	175.6	276.4			
p-cymene (**1k**)	−3.0	183.6	272.2	−7.4[g]	173.8[d]	215.9
allylbenzene (**1l**)	33.2	225.0	277.4			

[a] $\Delta_f H°(H^-) = 85.58$ kcal mol^{-1} (AM1). [b] $\Delta_f H°(H^-) = 34.7$ kcal mol^{-1}, from ref 10. [c] From ref 10. [d] From ref 11. [e] Calculated with $\Delta_f H°$(arene) from ref 10, proton affinities for arenes from ref 12a, and $\Delta_f H°(H^+) = 365.7$ kcal mol^{-1} from ref 10. [f] Calculated from $\Delta_f H°$(**1c**) = 20.13 kcal mol^{-1} in the condensed phase plus a vaporization enthalpy of 13 kcal mol^{-1} as for 1,2,3,4-tetrahydronaphthalene, from ref 13. [g] From ref 13.

to affect $\Delta G^‡$ differently as identical changes of $\Delta G°$ due to variation of the acid. Bernasconi's principle of nonperfect synchronization has been formulated to account for those findings.[6] The kinetic data reported in the preceding paper indicated that structural variations of allylic and benzylic hydride donors had remarkably small effects on hydride transfer rates, while these rates were strongly affected by variation of the hydride acceptors.[7] It was the goal of this work to search for the origin of these unexpected relationships.

Correlation between the Nucleophilicity Parameters *N* and Hydride Ion Affinities. Because of the problems to compare nucleophilic reagents of large structural variety with respect to a single reference electrophile, we have introduced eq 3, which allows one to compare nucleophilic reagents of widely varying reactivities.[8,9]

$$\log k(20\ °C) = s(N + E) \qquad (3)$$

where *s* is the nucleophile-specific slope parameter, *N* is the nucleophilicity parameter, and *E* is the electrophilicity parameter.

Because *s* has been found to be close to 1 for several CH hydride donors,[7] the relative reactivities of different hydride donors ($\Delta \log k$) can be substituted by ΔN, and the slope of a correlation (2.303*RT*)*N* versus hydride ion affinity (HIA) of the resulting carbocations corresponds to Bell−Evans−Polanyi's B (eq 1) or Hammond−Leffler's α (eq 2). The low quality of the correlation between *N* and calculated hydride affinities (AM1, Table 1) as well as the small slope of this correlation (Figure 1) confirm, in agreement with the conclusions drawn in the preceding article, that hydride transfer rates are not predominantly controlled by the stabilization of the carbocations produced.

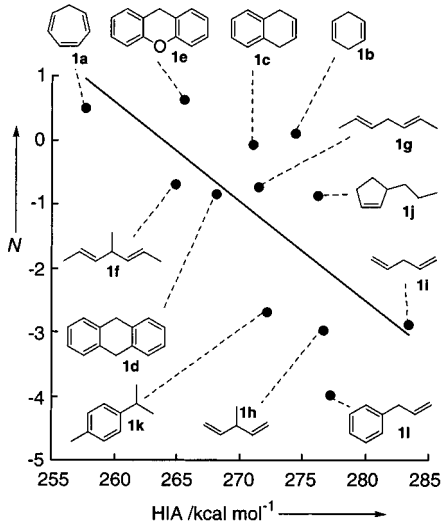

Figure 1. Correlation between the hydride reactivity *N* of various hydrocarbons (CH_2Cl_2, 20 °C) and the calculated (AM1) hydride ion affinities HIA of the resulting carbenium ions ($N = -0.1608$ HIA + 42.43; $r = 0.6941$).

Disregarding the large scatter of the correlation in Figure 1, one can derive from its slope that roughly 20% of the differences in the thermodynamic driving force are found as differences in the hydride transfer rates ($2.303RT \times 0.1608 = 0.216$). An even smaller value (15%) is calculated, when the correlation between *N* and the six experimentally available hydride affinities (Table 1) is considered. This finding sharply contrasts the situation in S_N1 reactions, where approximately 89% of the differences of the heats of ionization in solution[14] and 53% of the differences of the gas-phase hydride affinities are observable in the transition states of the ethanolysis reactions.[15]

(5) (a) Bordwell, F. G.; Boyle, W. J., Jr.; Hautala, J. A.; Yee, K. C. *J. Am. Chem. Soc.* **1969**, *91*, 4002−4003. (b) Marcus, R. A. *J. Am. Chem. Soc.* **1969**, *91*, 7224−7225. (c) Pross, A. *Adv. Phys. Org. Chem.* **1977**, *14*, 69−132; see refs on pp 93−96. (d) Lewis, E. S.; Hu, D. D. *J. Am. Chem. Soc.* **1984**, *106*, 3292−3296. (e) Wiseman, F.; Kestner, N. R. *J. Phys. Chem.* **1984**, *88*, 4354−4358. (f) Lewis, E. S. *J. Phys. Chem.* **1986**, *90*, 3756−3759. (g) Yamataka, H.; Nagase, S. *J. Org. Chem.* **1988**, *53*, 3232−3238. (h) Bunting, J. W.; Stefanidis, D. *J. Am. Chem. Soc.* **1989**, *111*, 5834−5839. (i) Pross, A.; Shaik, S. *New J. Chem.* **1989**, *13*, 427−433. (j) Arnaut, L. G. *J. Phys. Org. Chem.* **1991**, *4*, 726−745. (k) Guthrie, J. P. *J. Am. Chem. Soc.* **1996**, *118*, 12886−12890. (l) Lee, W. T.; Masel, R. I. *J. Phys. Chem. A* **1998**, *102*, 2332−2341. (m) Yamataka, H.; Mustanir; Mishima, M. *J. Am. Chem. Soc.* **1999**, *121*, 10223−10224. (n) Shaik, S.; Shurki, A. *Angew. Chem.* **1999**, *111*, 616−657; *Angew. Chem., Int. Ed.* **1999**, *38*, 586−625. (o) Toteva, M. M.; Richard, J. P. *J. Am. Chem. Soc.* **2000**, *122*, 11073−11083. (p) See also ref 28.

(6) Bernasconi, C. F. *Adv. Phys. Org. Chem.* **1992**, *27*, 119−238 and references therein.

(7) Mayr, H.; Lang, G.; Ofial, A. R. *J. Am. Chem. Soc.* **2002**, *124*, 4076−4083.

(8) (a) Mayr, H.; Patz, M. *Angew. Chem.* **1994**, *106*, 990−1010; *Angew. Chem., Int. Ed. Engl.* **1994**, *33*, 938−955. (b) Mayr, H.; Kuhn, O.; Gotta, M. F.; Patz, M. *J. Phys. Org. Chem.* **1998**, *11*, 642−654. (c) Mayr, H.; Patz, M.; Gotta, M. F.; Ofial, A. R. *Pure Appl. Chem.* **1998**, *70*, 1993−2000. (d) Mayr, H.; Bug, T.; Gotta, M. F.; Hering, N.; Irrgang, B.; Janker, B.; Kempf, B.; Loos, R.; Ofial, A. R.; Remennikov, G.; Schimmel, H. *J. Am. Chem. Soc.* **2001**, *123*, 9500−9512.

(9) Lucius, R.; Loos, R.; Mayr, H. *Angew. Chem.* **2002**, *114*, 97−102; *Angew. Chem., Int. Ed.* **2002**, *41*, 91−95.

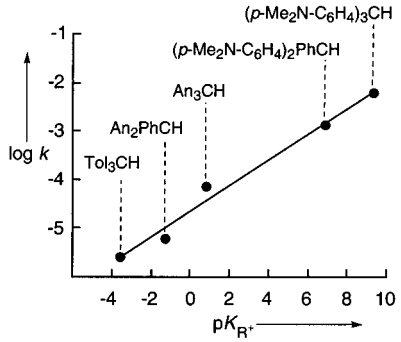

Figure 2. Correlation between the rates of hydride transfer (CH_3CN, 23 °C) from various triarylmethanes to the tritylium ion and pK_{R^+} of the resulting carbenium ions (log k = 0.263 pK_{R^+} − 4.652, r = 0.992).[16] An = p-H_3CO−C_6H_4; Tol = p-H_3C−C_6H_4.

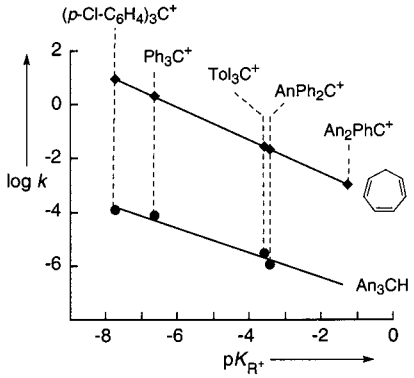

Figure 3. Correlation between the rates of hydride transfer (CH_3CN, 23 °C) from cycloheptatriene (log k = −0.61 pK_{R^+} − 3.73, r = 0.999) and tris(p-anisyl)methane (log k = −0.46 pK_{R^+} − 7.33, r = 0.983) to tritylium ions and the corresponding pK_{R^+} values.[16] An = p-H_3CO−C_6H_4.

It may be argued that the small slope of the correlation in Figure 1 is due to the fact that kinetic data in solution are correlated with thermodynamic data referring to the gas phase. The following examples show, however, that similar conclusions can be drawn from rate-equilibrium relationships, where kinetic and thermodynamic data refer to the solution.

McDonough[16] found a good correlation between hydride abstraction rates from p-substituted triarylmethanes and pK_{R^+} of the tritylium ions produced during this reaction (Figure 2). Because the rate and equilibrium constants correlated in Figure 2 refer to almost the same temperature, the slope of this correlation (0.263) can directly be compared with the slope derived from Figure 1. One again finds that only a small percentage (26%, slope in Figure 2) of the change of the reaction free energy caused by variation of the hydride donor is found in the transition states of the hydride transfer reactions. In contrast, (log k)/pK_{R^+} correlations that refer to reaction series, in which the hydride acceptors (tritylium[16] or 9-arylfluorenylium[17] ions) are altered, show much higher slopes (Figures 3 and 4).

In all reaction series, we observe the same phenomenon: a small percentage of $\delta\Delta G°$ (15−26%) is encountered in the

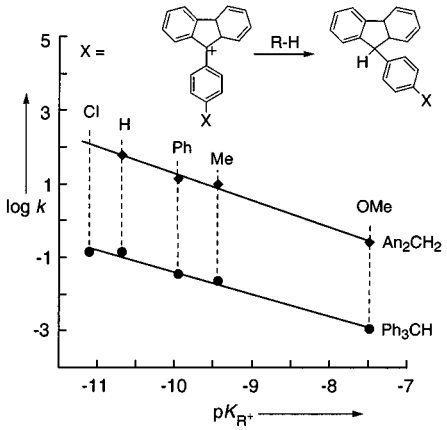

Figure 4. Correlation between the rates of hydride transfer (CF_3COOH, 30 °C) from bis(p-anisyl)methane (log k = −0.73 pK_{R^+} − 6.02, r = 0.995) and triphenylmethane (log k = −0.60 pK_{R^+} − 7.40, r = 0.993) to 9-arylfluorenylium ions and the corresponding pK_{R^+} values.[17]

Scheme 1

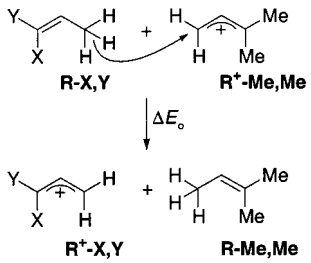

transition states of the hydride transfer reactions when the hydride donor is varied, while a high percentage of $\delta\Delta G°$ (46−73%) is found in the transition states when the hydride acceptor is varied. To rationalize this behavior, the transition structures of the hydride transfer reactions were calculated by semiempirical, ab initio, and DFT MO methods. Because the identification of electronic effects is most straightforward when the steric situation at the reaction centers is kept constant, we have selected the model reaction shown in Scheme 1, which refers to hydride transfer processes of widely differing driving forces, while the centers of the reactions remain unchanged.

Quantum Chemical Calculations of Reactants and Transition Structures. Computational Methods. All compounds (substituted allyl cations and the corresponding propenes), the transition states for hydride transfer, and the molecular complexes (van der Waals complexes) were calculated at various levels of theory. First, all structures were optimized using the semiempirical method AM1[18] of the program package MOPAC93[19] (no symmetry constraint was applied). Then, geometry optimizations using the RHF/6-31+G(d,p) basis set of the *Gaussian 98* program package[20] were performed. Frequency calculations for all stationary points were carried out to characterize them either as minima (NIMAG = 0) or as transition states (NIMAG = 1). Zero point energies are given

(10) NIST Chemistry WebBook (NIST Standard Reference Database Number 69−July 2001 Release): http://webbook.nist.gov.
(11) Lias, S. G.; Bartmess, J. E.; Liebman, J. F.; Holmes, J. L.; Levin, R. D.; Mallard, W. G. *J. Phys. Chem. Ref. Data, Suppl. 1* **1988**.
(12) (a) Aue, D. H.; Guidoni, M.; Betowski, L. D. *Int. J. Mass Spectrom.* **2000**, *201*, 283−295. (b) Aue, D. H. In *Dicoordinated Carbocations*; Rappoport, Z., Stang, P. J., Eds.; Wiley: New York, 1997; Chapter 3.
(13) Pedley, J. B.; Naylor, R. D.; Kirby, S. P. *Thermochemical Data of Organic Compounds*, 2nd ed.; Chapman & Hall: London, 1986.
(14) Arnett, E. M.; Petro, C.; Schleyer, P. v. R. *J. Am. Chem. Soc.* **1979**, *111*, 522−526.
(15) Mayr, H. In *Cationic Polymerizations: Mechanisms, Synthesis, and Applications*; Matyjaszewski, K., Ed.; Marcel Dekker: New York, 1996; Chapter 2.
(16) McDonough, L. M. Ph.D. Thesis, University of Washington, 1960.
(17) Bethell, D.; Hare, G. J.; Kearney, P. A. *J. Chem. Soc., Perkin Trans. 2* **1981**, 684−691.
(18) Dewar, M. J. S.; Zoebisch, E. G.; Healy, E. F.; Stewart, J. J. P. *J. Am. Chem. Soc.* **1985**, *107*, 3902−3909.
(19) Stewart, J. J. P. *MOPAC93*; Fujitsu Ltd. 1993.

Table 2. Hydride Affinities (kcal mol^{-1}) of **R$^+$−H**,**Me** and **R$^+$−Me**,**Me** Calculated on Various Levels of Theory Compared to the Experimental Values

method[a]	R$^+$–H,Me	R$^+$–Me,Me
AM1//AM1	295.21	287.24
RHF/6-31+G(d,p)//RHF/6-31+G(d,p)	267.54	258.37
MP2/6-31+G(d,p)//RHF/6-31+G(d,p)	287.37	278.58
B3LYP/6-31+G(d,p)//B3LYP/6-31+G(d,p)	278.11	268.36
G2MP2	259.55	250.16
G3MP2	247.37	237.83
experimental	238.9[b]	230.4[b]

[a] Ab initio and DFT hydride affinities refer to $\Delta E_0 = E_{tot} + ZPE$. [b]From ref 12b.

unscaled, since scaling factors of 0.92 (tested for some examples) give reaction energies and free energies (Scheme 1, Tables 3−8) which deviate less than 0.2 kcal mol^{-1} from the unscaled values. For the calculation of hydride affinities, a scaling factor of 0.92 was used.[21] The energies discussed (E_0) are the sum of single point MP2/6-31+G(d,p)//RHF/6-31+G(d,p) calculations and zero point corrections (0 K). Free energies ($\Delta G°$, 298.15 K, 1.0 atm) are the sum of the MP2 single point calculations and the thermal corrections to Gibbs' free energy as obtained from the frequency calculations. For calibrating purposes some of the systems were calculated employing the B3LYP/6-31+G(d,p) DFT method as well as G2MP2[22a] and G3MP2.[22b] Only the latter method yields hydride affinities close to the experimental values (Table 2), while all other methods give values which are 20−60 kcal mol^{-1} too high, probably because of the problems with calculation of the energy of the hydride ion.

The activation energies for these hydride transfer reactions also depend highly on the level of computation as indicated by Figure 5. RHF methods (AM1, RHF/6-31+G(d,p)) greatly overestimate the activation barriers since unusually large correlation energy effects are observed in the transition states. Fortunately, the MP2/6-31+G(d,p)//RHF/6-31+G(d,p) energies do not differ significantly from the G3MP2 results, allowing us to use this much less expensive method. However, it is well known[23] that the DFT method B3LYP/6-31+G(d,p) underestimates the activation barriers, resulting in hydrido-bridged minima for the less stabilized systems. Whereas the RHF/6-31+G(d,p) transition structures generally relax to give van der Waals complexes, some of the DFT transition states relax with formation of a new CC-bond (attack of the allyl cation at the CC-double bond of the substituted propene). The basis set superposition error (BSSE) appears to be negligible since an increase of the basis set (6-31+G(2d,p), 6-31+G(3d,2p)) did not alter the relative energies significantly.

(20) Frisch, M. J.; Trucks, G. W.; Schlegel, H. B.; Scuseria, G. E.; Robb, M. A.; Cheeseman, J. R.; Zakrzewski, V. G.; Montgomery, J. A., Jr.; Stratmann, R. E.; Burant, J. C.; Dapprich, S.; Millam, J. M.; Daniels, A. D.; Kudin, K. N.; Strain, M. C.; Farkas, O.; Tomasi, J.; Barone, V.; Cossi, M.; Cammi, R.; Mennucci, B.; Pomelli, C.; Adamo, C.; Clifford, S.; Ochterski, J.; Petersson, G. A.; Ayala, P. Y.; Cui, Q.; Morokuma, K.; Malick, D. K.; Rabuk, A. D.; Raghavachari, K.; Foresman, J. B.; Cioslowski, J.; Ortiz, J. V.; Stefanov, B. B.; Liu, G.; Liashenko, A.; Piskorz, P.; Komaromi, I.; Gomperts, R.; Martin, R. L.; Fox, D. J.; Keith, T.; Al-Laham, M. A.; Peng, C. Y.; Nanayakkara, A.; Gonzalez, C.; Challacombe, M.; Gill, P. M. W.; Johnson, B. G.; Chen, W.; Wong, M. W.; Andres, J. L.; Head-Gordon, M.; Replogle, E. S.; Pople, J. A. *Gaussian 98*; Gaussian, Inc.: Pittsburgh, PA, 1998.
(21) Scott, A. P.; Radom, L. *J. Phys. Chem.* **1996**, *100*, 16502−16513.
(22) (a) Curtiss, L. A.; Raghavachari, K.; Pople, J. A. *J. Chem. Phys.* **1993**, *98*, 1293−1298. (b) Curtiss, L. A.; Redfern, P. C.; Raghavachari, K.; Rassolov, V.; Pople, J. A. *J. Chem. Phys.* **1999**, *110*, 4703−4709.
(23) (a) Johnson, B. G.; Gonzalez, C. A.; Gill, P. M. W.; Pople, J. A. *Chem. Phys. Lett.* **1994**, *221*, 100−108. (b) Csonka, G. I.; Johnson, B. G. *Theor. Chem. Acc.* **1998**, *99*, 158−165.

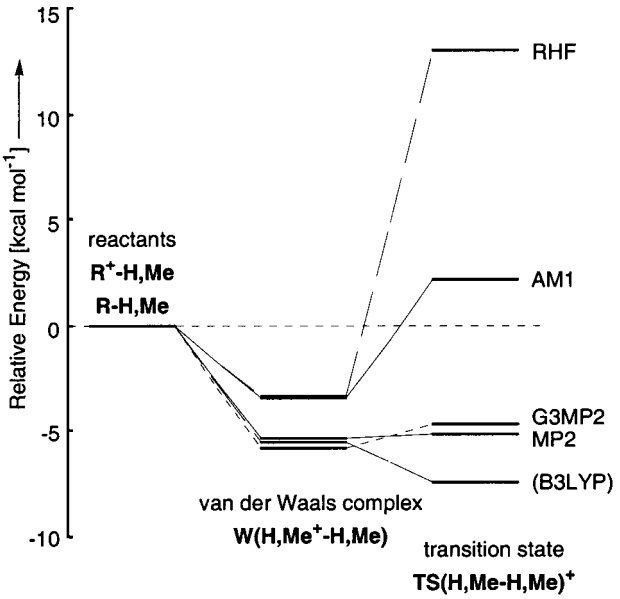

Figure 5. Relative energies of the van der Waals complexes and transition states for the degenerate reaction of **R$^+$−H**,**Me** with **R−H**,**Me** calculated on various levels of theory. B3LYP gives a minimum for the hydrido bridged species (NIMAG = 0) and is therefore marked in parentheses. For the RHF, MP2, and B3LYP calculations, the 6-31+G(d,p) basis set was used.

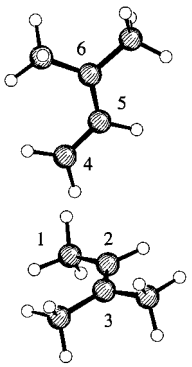

Figure 6. Molecular structure of the van der Waals complex **W(Me**,**Me$^+$−Me**,**Me)** (RHF/6-31+G(d,p)//RHF/6-31+G(d,p)).

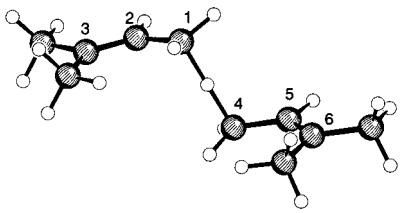

Figure 7. Molecular structure of transition state **TS(Me**,**Me−Me**,**Me)$^+$**. Bond lengths H−C1 = H−C4: 1.2898 Å (RHF/6-31+G(d,p)//RHF/6-31+G(d,p)).

For the calculation of the reaction pathways, the coplanar anti-arrangement of the bonds C1/C2 and C4/C5 (see Figure 7) was chosen as starting geometry to avoid attack of the 1,1-dimethylallyl cation at the CC-double bond or the lone pairs of X and Y. Successive reduction of the distance between the allylic hydrogen (1-H) and the acceptor carbon C4 leads to the transition state. Intrinsic reaction path calculations (IRC) as well as full optimizations starting from the slightly disturbed transition state geometries led to molecular complexes of the van der Waals type which represent the true minima of these parts of the potential energy surfaces.

Table 3. Total Energies (au)[a] and Zero Point Energies (kcal mol^{-1}) of the Hydride Donors **R**−**X**,**Y** and the Resulting Carbenium Ions **R**$^+$−**X**,**Y** and Calculated Reaction Energies (kcal mol^{-1}) for the Hydride Transfer of Scheme 1 (MP2/6-31+G(d,p)//RHF/6-31+G(d,p))

X,Y	E_{tot}(**R**–**X**,**Y**)	ZPE(**R**–**X**,**Y**)	E_{tot}(**R**$^+$–**X**,**Y**)	ZPE(**R**$^+$–**X**,**Y**)	ΔE_0	$\Delta_r G°$(25°C)
Me,NH_2	−211.90589	83.78	−211.07090	77.77	−33.22	−32.86
OH,OH	−267.59849	60.22	−266.73547	53.67	−16.17	−15.80
Me,OH	−231.73838	75.29	−230.87129	68.75	−13.60	−13.79
H,OH	−192.54957	56.43	−191.66885	50.38	−4.56	−2.32
Me,Me	−195.88350	90.71	−194.99280	82.95	0.00	0.00
H,Me	−156.69735	72.00	−155.79273	64.31	8.79	8.72

[a] 1 au = 627.51 kcal mol^{-1}.

Table 4. Total Energies (au)[a] and Zero Point Energies (kcal mol^{-1}) of the van der Waals Complexes **W**(**X**,**Y**$^+$−**X**,**Y**) Obtained from **R**$^+$−**X**,**Y** and **R**−**X**,**Y** (MP2/6-31+G(d,p)//RHF/6-31+G(d,p)) and the Corresponding Reaction Energies and Free Energies

X,Y	E_{tot}	ZPE	ΔE_0	$\Delta_r G°$(25°C)
Me,NH_2	−423.01183	163.01	−20.53	−10.66
Me,OH	−462.63284	145.01	−13.57	−4.25
Me,Me	−390.88600	174.00	−5.74	0.53
H,Me	−312.49923	136.74	−5.31	0.68

[a] 1 au = 627.51 kcal mol^{-1}.

Reaction Energies. According to Table 3, the reaction energies for the hydride abstractions depicted in Scheme 1 range from −33.2 kcal mol^{-1} for the formation of the highly stabilized 1-amino-1-methylallyl cation to +8.8 kcal mol^{-1} for the formation of the less stabilized 1-methylallyl cation. Almost the same values were calculated for the reaction free energies.

van der Waals Complexes. For the hydrocarbon systems (X,Y = Me and/or H), complexation energies of 5−6 kcal mol^{-1} are calculated (Table 4), in good agreement with experience.[24] Systems with OH or NH_2 substituents, however, give higher complexation energies (13−21 kcal mol^{-1}) due to hydrogen bonding as shown for the reactions of **R**$^+$−**X**,**Y** with **R**−**X**,**Y** in Table 4. Particularly the loss of translational degrees of freedom accounts for the 6−10 kcal mol^{-1} difference between ΔE_0 and $\Delta_r G°$.

In the van der Waals complex **W(Me**,**Me**$^+$−**Me**,**Me)** obtained from **R**−**Me**,**Me** and **R**$^+$−**Me**,**Me** (Figure 6), the plane of the allyl cation is located perpendicular to the plane of the olefin, with the shortest CC-distances of 3.79 and 3.93 Å between C4 of the cation and C2 and C3 of the olefin. The shortest CH-distances between cation and olefin are 2.75 (4H−C2) and 2.89 Å (4H−C3) indicating substantial CH interaction. The distance between the migrating 1H and the acceptor center C4 is considerably longer (3.74 Å).

The van der Waals interactions are eliminated in the following analyses by considering the activation energies with respect to the sum of the starting materials and not relative to the energies of the van der Waals complexes.

Transition Structures for Hydride Transfer. The transition structures (Figure 7) have explicitly been optimized and demonstrated to be saddle points on the energy hypersurface; they possess one and only one negative force constant. These transition structures have rather small relative energies ($\Delta E^‡$) with respect to the separated reactants ranging from −8 to +10 kcal mol^{-1}.

As a consequence of the initial formation of van der Waals complexes, stationary points can also be found for transition

Table 5. Total Energies (au)[a] and Zero Point Energies (kcal mol^{-1}) of the Activated Complexes **TS(Me,Me**−**X,Y)**$^+$ and Activation Barriers $\Delta E^‡$ and $\Delta G^‡$ (kcal mol^{-1}) for the Hydride Transfer Reactions of Scheme 1 (MP2/6-31+G(d,p)//RHF/6-31+G(d,p))

			forward reaction		backward reaction	
X,Y	E_{tot}	ZPE	$\Delta E^‡$[b]	$\Delta G^‡$ (25 °C)[c]	$\Delta E^‡$[d]	$\Delta G^‡$ (25 °C)[c]
OH,OH	−462.59993	142.10	−6.50	3.65	9.67	19.45
Me,OH	−426.74071	157.55	−6.67	3.59	6.93	17.38
H,OH	−387.54743	139.08	−3.49	8.46	1.08	10.77
Me,Me	−390.88004	172.51	−3.49	6.50	−3.49	6.50
H,Me	−351.68742	153.95	0.71	10.56	−8.08	1.84

[a] 1 au = 627.51 kcal mol^{-1}. [b] $\Delta E^‡$(forward) = E_0(**TS(Me**,**Me**−**X**,**Y)**$^+$) − E_0(**R**−**X**,**Y**) − E_0(**R**$^+$−**Me**,**Me**). [c] For calculation see footnotes d and e of Table 10. [d] $\Delta E^‡$(backward) = E_0(**TS(Me**,**Me**−**X**,**Y)**$^+$) − E_0(**R**−**Me**,**Me**) − E_0(**R**$^+$−**X**,**Y**).

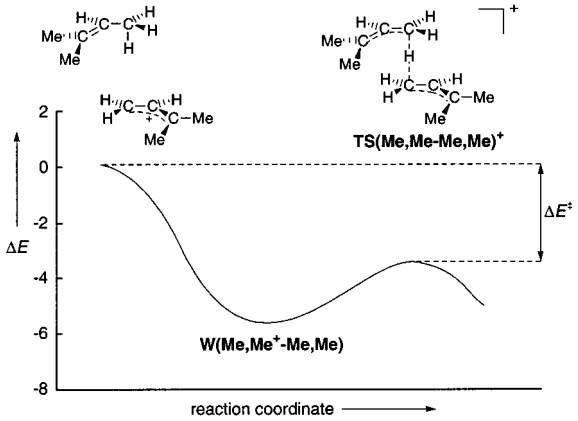

Figure 8. Energy diagram for the reaction of **R**−**Me**,**Me** with **R**$^+$−**Me**,**Me**.

structures which are energetically more favorable than the reactants (Table 5, Figure 8). The absolute barriers with respect to the van der Waals complexes range from 0 to 26 kcal mol^{-1}. However, the highly exothermic reactions of **R**−**Me**,**NH**$_2$ and **R**−**NH**$_2$,**NH**$_2$ with **R**$^+$−**Me**,**Me** proceed to the products without barrier, and transition states could not be located for these reactions.

As depicted for **TS(Me**,**Me**−**Me**,**Me)**$^+$ in Figure 7, transition structures with almost linear arrangements of C1−H−C4 were calculated for all reactions listed in Table 5 (Table 6). Analogously, C−H−C angles of 180° and 160° were calculated for (*t*Bu−H−*t*Bu)$^+$ and (*i*Pr−H−*i*Pr)$^+$, while this angle reduces to 133° and 106° for (Et−H−Et)$^+$ and (Me−H−Me)$^+$, respectively.[25a,b]

Table 6 and Figure 9 show that the highly exothermic reaction of **R**$^+$−**Me**,**Me** with 1,1-dihydroxypropene (**R**−**OH**,**OH**) pro-

(24) (a) Kim, K. S.; Tarakeshwar, P.; Lee, J. Y. *Chem. Rev.* **2000**, *100*, 4145−4186. (b) Chałasiński, G.; Szczęśniak, M. M. *Chem. Rev.* **2000**, *100*, 4227−4252.

(25) (a) Frash, M. V.; Solkan, V. N.; Kazansky, V. B. *J. Chem. Soc., Faraday Trans.* **1997**, *93*, 515−520. (b) Boronat, M.; Viruela, P.; Corma, A. *J. Phys. Chem. B* **1997**, *101*, 10069−10074. (c) Boronat, M.; Viruela, P.; Corma, A. *J. Phys. Chem. B* **1999**, *103*, 7809−7821.

Table 6. Bond Angles and Bond Lengths in the Transition States of the Hydride Transfer Reactions of Scheme 1 (RHF/6-31+G(d,p))

X,Y	ΔE_0, kcal mol^{-1}	β(C1–H–C4)	d(H–C1), Å	d(H–C4), Å
OH,OH	−16.17	177.87°	1.2429	1.3579
Me,OH	−13.60	176.45°	1.2464	1.3633
H,OH	−4.56	178.42°	1.2764	1.3138
Me,Me	0.00	179.82°	1.2898	1.2898
H,Me	8.79	177.44°	1.3463	1.2413

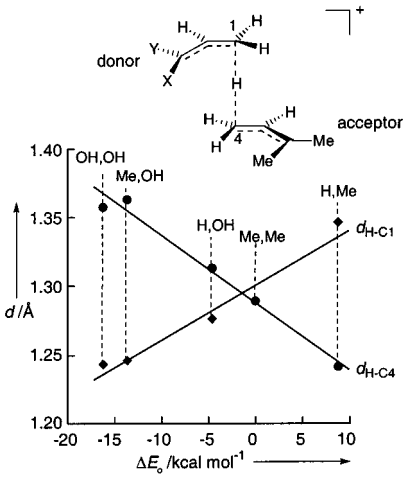

Figure 9. CH-bond lengths in the transition states of the hydride transfer reactions of Scheme 1 (RHF/6-31+G(d,p)).

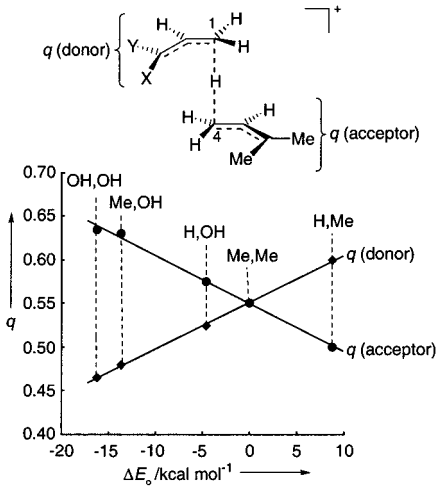

Figure 10. Distribution of charges q (in multiples of electron charge) in the transition states of the hydride transfer reactions of Scheme 1 (RHF/6-31+G(d,p), Mulliken analysis).

ceeds through an early transition state closely resembling the reactants, while the endothermic reaction of $\mathbf{R}^+-\mathbf{Me},\mathbf{Me}$ with $\mathbf{R}-\mathbf{H},\mathbf{Me}$ proceeds through a late transition state in which the bond being formed (d_{H-C4} = 1.24 Å) is already shorter than the bond being broken (d_{H-C1} = 1.35 Å). In the symmetrical transition state of the thermoneutral reaction (X,Y = Me), the equal H−C1/C4 distances are 1.29 Å. The computational results thus are in perfect agreement with the expectations based on Hammond's postulate.[26]

The change from early to late transition states on the way from exothermic to endothermic reactions can also be seen in the charge distribution of the transition states (Mulliken analysis from the RHF/6-31+G(d,p)-optimizations, see Table S6 in the

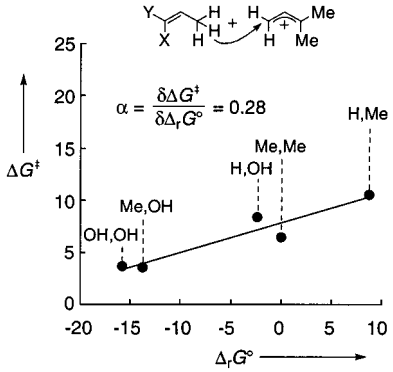

Figure 11. Brønsted plot for the forward reaction of Scheme 1 (variation of the hydride donor, MP2/6-31+G(d,p)//RHF/6-31+G(d,p), energies in kcal mol^{-1}).

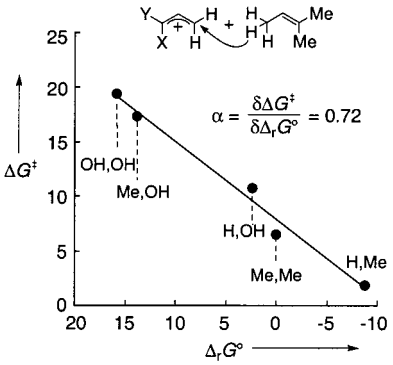

Figure 12. Brønsted plot for the backward reaction of Scheme 1 (variation of the hydride acceptor, MP2/6-31+G(d,p)//RHF/6-31+G(d,p), energies in kcal mol^{-1}).

Scheme 2

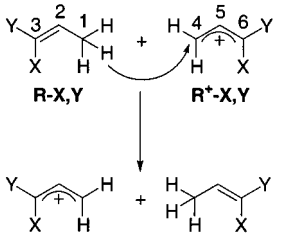

Supporting Information), when one considers the sum of the charges at the donor and the acceptor fragments (Figure 10) as indication for the progress of the reaction. Again in agreement with Hammond's postulate, the positive charge is predominantly localized at the acceptor fragment in the early transition state of the reaction of $\mathbf{R}^+-\mathbf{Me},\mathbf{Me}$ with $\mathbf{R}-\mathbf{OH},\mathbf{OH}$, while more charge is localized at the donor fragment in the late transition state of the corresponding reaction with $\mathbf{R}-\mathbf{H},\mathbf{Me}$ (Figure 10).

Let us now look at the relationship between $\Delta G^{\ddagger}$ and $\Delta_r G^{\circ}$ which corresponds to Leffler−Hammond's α as defined by eq 2. Figure 11 shows a fairly linear plot with a slope of 0.28. If α were taken as a measure for the position of the transition state, one would derive an early transition state for the whole reaction series, in marked contrast to the conclusions drawn from Figures 9 and 10.

Necessarily, for the reverse reaction (Figure 12) a high value of α is derived ($\alpha = 1 - 0.28 = 0.72$) which would be indicative of a late transition state according to the Leffler−Hammond postulate.

Table 7. Total Energies of the Transition States of the Degenerate Reactions, Their Zero Point Energies, Bond Lengths to the Migrating Hydrogen, Bond Angles, and NBO Charges at the Migrating Hydrogen in the Transition States **TS(X,Y−X,Y)**$^+$ (MP2/6-31+G(d,p)//RHF/6-31+G(d,p))

X,Y	E_{tot}, au[a]	ZPE, kcal mol^{-1}	d(H–C1) = d(H–C4), Å	β(C1–H–C4)	NBO charges[b]
Me,NH_2	−422.96419	158.95	1.3142	176.63°	+0.151
OH,OH	−534.33192	112.00	1.3066	172.26°	+0.153
Me,OH	−462.60465	142.70	1.3044	175.24°	+0.147
H,OH	−384.21550	105.71	1.2981	178.63°	+0.145
Me,Me	−390.88004	172.51	1.2898	179.82°	+0.144
H,Me	−312.49662	135.27	1.2847[c]	174.66°[d]	+0.142

[a] 1 au = 627.51 kcal mol^{-1}. [b] According to ref 30. [c] d(H−C1) = d(H−C4) = 1.2856 Å at MP2(Full)/6-31G*//MP2(Full)/6-31G*. [d] β(C1−H−C4) = 178.65° at MP2(Full)/6-31G*//MP2(Full)/6-31G*.

Table 8. Selected Bond Lengths (Å) of the Carbon Skeleton of the Hydride Donors **R**−**X**,**Y**, of the Hydride Acceptors **R**$^+$−**X**,**Y**, and of the Transition States **TS**(**X**,**Y**−**X**,**Y**)$^+$ of the Degenerate Reactions in Scheme 2 According to MP2/6-31+G(d,p)//RHF/6-31+G(d,p)

	R–X,Y		R$^+$–X,Y		TS(X,Y–X,Y)$^+$	
X,Y	d(C1–C2)	d(C2–C3)	d(C4–C5)	d(C5–C6)	d(C1–C2)	d(C2–C3)
Me,NH_2	1.5052	1.3293	1.3302	1.4544	1.4261	1.3722
OH,OH	1.5019	1.3161	1.3340	1.4370	1.4280	1.3531
Me,OH	1.5036	1.3231	1.3382	1.4313	1.4340	1.3540
H,OH	1.5031	1.3175	1.3448	1.4103	1.4383	1.3439
Me,Me	1.5051	1.3277	1.3496	1.4175	1.4484	1.3478
H,Me[a]	1.5032	1.3227	1.3604	1.3927	1.4523	1.3379

[a] At MP2(Full)6-31G*//MP2(Full)/6-31G* the following bond lengths (Å) were obtained:1.4975, 1.3385, 1.3714, 1.3967, 1.4375, 1.3591.

In agreement with the experimental results discussed in the beginning, the calculations also lead to the conclusion that donor variation has a small influence on the activation free energy ($\alpha = 0.28$, Figure 11), while acceptor variation has a large influence ($\alpha = 0.72$, Figure 12).

The fact that Leffler−Hammond's α cannot be related to the location of the transition state is best illustrated by the degenerate reaction of **R**−**Me**,**Me** with **R**$^+$−**Me**,**Me**. By looking at this reaction as a representative of the series in Figure 11 one would derive an early transition state, whereas one would derive a late transition state for the same reaction when one looks at it as part of the reaction series of Figure 12. How can one explain the different magnitude of α as one analyzes Scheme 1 in the forward or backward sense?

Marcus Treatment of the Quantum Chemical Results. An explanation for these relationships is provided by Marcus theory which derives the activation free energy of a reaction $\Delta G^{\ddagger}$ from its intrinsic barrier $\Delta G_0^{\ddagger}$ and the reaction free energy $\Delta_r G°$ (eq 4).[27]

$$\Delta G^{\ddagger} = \Delta G_0^{\ddagger} + 0.5\Delta_r G° + ((\Delta_r G°)^2/16\Delta G_0^{\ddagger}) \qquad (4)$$

The work term of the Marcus equation can be neglected in ion−molecule reactions, because Coulomb interactions are small in these cases. While the intrinsic barrier may directly be measurable for degenerate reactions ($\Delta G^{\ddagger} = \Delta G_0^{\ddagger}$), $\Delta G_0^{\ddagger}$ is not directly accessible for nondegenerate reactions and is calculated as the arithmetic mean of the intrinsic barriers of the corresponding degenerate reactions (eq 5).[27,28]

$$(\Delta G_0^{\ddagger})_{ij} = 0.5((\Delta G_0^{\ddagger})_{ii} + (\Delta G_0^{\ddagger})_{jj}) \qquad (5)$$

Table 9. Hydride Affinities of the Allyl Cations **R**$^+$−**X**,**Y** and Intrinsic Barriers of the Degenerate Reactions in Scheme 2 (in kcal mol^{-1}; According to MP2/6-31+G(d,p)//RHF/6-31+G(d,p))

X,Y	HIA (G3MP2)	$\Delta E^{\ddagger}$	$(\Delta G_0^{\ddagger})_{ii}$
Me,NH_2	204.24	5.30	14.95
OH,OH	220.60	−0.62	10.76
Me,OH	224.02	1.81	12.43
H,OH	233.69	0.72	12.47
Me,Me	237.83	−3.49	6.50
H,Me	247.37	−5.14	4.71

To derive the intrinsic barriers according to eq 5, we have performed ab initio calculations on the degenerate hydride transfer reactions shown in Scheme 2.

As shown above for the nondegenerate reactions (Table 6), the arrangement C1−H−C4 is also almost linear in the transition structures of the degenerate reactions (Table 7), and the distance H−C1/4 decreases noticeably as the stabilization of the allyl cations is reduced. The increasing tightness of the bonding to the migrating hydrogen in the transition structures **TS(X,Y−X,Y$^+$)** is accompanied by an elongation of the C1−C2 (=C4−C5) bond and a shortening of the C2−C3 (=C5−C6) bond, that is, an increasing bond alternation from top to bottom of Table 8.

Table 9 shows the decrease of the intrinsic barriers with increasing hydride affinities of the corresponding allyl cations; that is, the intrinsic barriers decrease with decreasing stabilization of the carbocations involved. Analogously, the tendency to yield hydrido-bridged carbocations [R−H−R]$^+$ was calculated to increase in the series *t*Bu < *i*Pr < Et < Me.[25] In accord with these findings, NMR studies in superacidic solution revealed hydrido-bridging in cycloalkyl cations to be more pronounced in secondary than in tertiary carbocations.[29]

The intrinsic barriers $(\Delta G_0^{\ddagger})_{ii}$ of Table 9 can now be combined with the reaction free energies $\Delta_r G°$ in Table 3 for calculating $\Delta G^{\ddagger}$ for the forward and backward reactions of Scheme 1 using the Marcus formalism (eqs 4 and 5). It can be seen in Table 10 that the activation free energies derived from Marcus theory closely agree with the activation free energies directly calculated by MP2. The different slopes of the plots in Figures 11 and 12 thus find a straightforward explanation.

When 1,1-dihydroxy-propene (**R**−**OH**,**OH**) is replaced by 2-butene (**R**−**H**,**Me**), $\Delta_r G°$ increases by 24.5 kcal mol^{-1} (Figure 11), the same amount that $\Delta_r G°$ of the backward reactions is reduced (Figure 12). In both reaction series the intrinsic barrier

(26) Analogous changes of the transition structures have been calculated for hydrogen radical abstractions from Me−H, Et−H, *i*Pr−H, and *t*Bu−H by H: ref 5g.

(27) Marcus, R. A. *J. Phys. Chem.* **1968**, *72*, 891−899.

(28) (a) Kreevoy, M. M.; Lee, I.-S. H. *J. Am. Chem. Soc.* **1984**, *106*, 2550−2553. (b) Kreevoy, M. M.; Ostović, D.; Lee, I.-S. H.; Binder, D. A.; King, G. W. *J. Am. Chem. Soc.* **1988**, *110*, 524−530. (c) Lee, I.-S. H.; Ostović, D.; Kreevoy, M. *J. Am. Chem. Soc.* **1988**, *110*, 3989−3993. (d) Kim, D.; Lee, I.-S. H.; Kreevoy, M. M. *J. Am. Chem. Soc.* **1990**, *112*, 1889−1894. (e) Kreevoy, M. M.; Kotchevar, A. T. *J. Am. Chem. Soc.* **1990**, *112*, 3579−3583. (f) Kim, Y.; Truhlar, D. G.; Kreevoy, M. M. *J. Am. Chem. Soc.* **1991**, *113*, 7837−7847. (g) Lee, I.-S. H.; Jeoung, E. H.; Kreevoy, M. M. *J. Am. Chem. Soc.* **1997**, *119*, 2722−2728. (h) Lee, I.-S. H.; Jeoung, E. H. *J. Org. Chem.* **1998**, *63*, 7275−7279. (i) Lee, I.-S. H.; Jeoung, E. H.; Kreevoy, M. M. *J. Am. Chem. Soc.* **2001**, *123*, 7492−7496.

(29) (a) Kirchen, R. P.; Sorensen, T. S. *J. Am. Chem. Soc.* **1979**, *101*, 3240−3243. (b) Kirchen, R. P.; Ranganayakulu, K.; Rauk, A.; Singh, B. P.; Sorensen, T. S. *J. Am. Chem. Soc.* **1981**, *103*, 588−596. (c) Sorensen, T. S. In *Stable Carbocation Chemistry*; Prakash, G. K. S., Schleyer, P. v. R., Eds.; Wiley: New York, 1997; pp 75−136.

Table 10. Indirectly (Marcus) and Directly Calculated Activation Free Energies (kcal mol^{-1}) for the Reaction of **R**$^+$−**Me**,**Me** with **R**−**X**,**Y** (Scheme 1)

			$\Delta G^{\ddagger}$(forward reaction)		$\Delta G^{\ddagger}$(backward reaction)	
X,Y	$\Delta_r G^{\circ}$[a]	$\Delta G_0^{\ddagger}$[b]	Marcus[c]	MP2[d]	Marcus[c]	MP2[e]
OH,OH	−15.80	8.63	2.54	3.65	18.34	19.45
Me,OH	−13.79	9.47	3.83	3.59	17.62	17.38
H,OH	−2.32	9.49	8.36	8.46	10.68	10.77
Me,Me	0.00	6.50	6.50	6.50	6.50	6.50
H,Me	8.72	5.61	10.82	10.56	2.10	1.84

[a] See data in Table 3. [b] Intrinsic barriers $\Delta G_0^{\ddagger} = (\Delta G_0^{\ddagger})_{ij}$ were calculated according to eq 5 from data in Table 9. [c] From $\Delta_r G^{\circ}$ and $\Delta G_0^{\ddagger}$ (columns 2 and 3 of this table) according to eq 4. [d] $\Delta G^{\ddagger} = G_{298}(\mathbf{TS(Me,Me-X,Y)}^+) - G_{298}(\mathbf{R}^+\mathbf{-Me,Me}) - G_{298}(\mathbf{R-X,Y})$. [e] $\Delta G^{\ddagger} = G_{298}(\mathbf{TS(Me,Me-X,Y)}^+) - G_{298}(\mathbf{R-Me,Me}) - G_{298}(\mathbf{R}^+\mathbf{-X,Y})$.

decreases by 3 kcal mol^{-1}, as one moves from **R**−**OH**,**OH** to **R**−**H**,**Me**. The moderate increase of the activation free energy when going from left to right in Figure 11 thus is due to the fact that the contribution of the increasing reaction enthalpy is partially compensated by the decreasing intrinsic barrier. In contrast, reaction free energy and intrinsic barrier are altered in the same sense when moving from X,Y = OH,OH to X,Y = H,Me in the backward reaction of Scheme 1, and thus are responsible for the high slope of the correlation in Figure 12.

It can thus be concluded that the strong dependence of hydride transfer rates on variation of the hydride acceptor is due to the fact that structural effects that increase the thermodynamic driving force lower the intrinsic barrier. The small dependence of hydride transfer rates on variation of the hydride donor, on the other hand, is due to the fact that factors that increase the thermodynamic driving force raise the intrinsic barrier and thus lead to a partial cancellation of both effects.

The variability of intrinsic barriers within reaction series has previously been demonstrated for hydride transfer reactions between NAD^+ analogues by Kreevoy et al.[28] We can now compare the results of Kreevoy's analysis with the calculated transition structures for hydride transfer reactions. Kreevoy and Lee[28a] showed that structural changes in either A_i^+ or A_jH that have similar effects on K_{ij} of eq 6 can have different effects on intrinsic reactivity and, consequently, on k_{ij}.

$$A_i^+ + A_jH \rightleftharpoons A_iH + A_j^+ \qquad (6)$$

If the in-flight hydrogen carries a full negative charge ($q = -1$), the differential quotient $\alpha = \delta(\ln k_{ij})/\delta(\ln K_{ij})$ should be 0 when A_i^+ is varied, and one would expect $\alpha = 1$ when A_jH is varied. Only if $q = 0$ should variations in K_{ij} have equal effects on k_{ij} independent of which reactant (A_i^+ or A_jH) is changed.

Application of this qualitative analysis on the reaction series shown in Figure 11 ($\alpha = 0.28$) and Figure 12 ($\alpha = 0.72$) leads to the conclusion that the in-flight hydrogen carries a positive partial charge. It has been suggested[28a] that the charge q of the in-flight H, which is related to the tightness parameter τ by eq 7, can experimentally be determined as the slope of a plot of ln k_{ii} against ln K_{ij}.

$$q = \tau - 1 = \delta(\ln k_{ii})/\delta(\ln K_{ij}) \qquad (7)$$

Replacement of ln k_{ii} and ln K_{ij} by the corresponding free energy terms listed in Tables 3 and 9 leads to the correlation shown in Figure 13, which indicates a positive partial charge

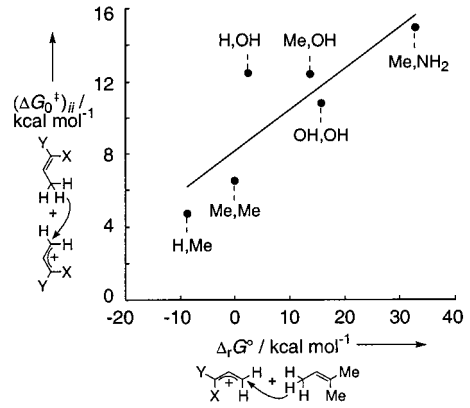

Figure 13. Correlation between the intrinsic barriers and the Gibbs reaction energies of a series of hydride acceptors toward a reference hydride donor [$(\Delta G_0^{\ddagger})_{ii} = 0.2256\Delta_r G^{\circ} + 8.1961$, $r = 0.8450$, $n = 6$].

of $q = +0.2$ on the in-flight hydrogen. In accord with these conclusions a positive charge ($q = +0.15$) on the migrating hydrogen is found in the calculated NBO charges[30] (Table 7).

These conclusions are in agreement with the results of our experimental investigations[7] and the experimental data presented in Figures 1−4. In contrast, a partially hydridic character has been derived for the in-flight hydrogen in hydride transfer reactions between NAD^+ analogues.[28] The difference may be a result of the lower hydride affinities of pyridinium ions as compared to those of the carbocations discussed above.

The less tight transition states of hydride transfer reactions between pyridinium derivatives can directly be seen in the C−H−C bond lengths of the hydrido bridge.[31] While Table 7 shows an elongation from 1.28 to 1.31 Å with increasing stabilization of the allyl cation, a value of 1.36 Å has been calculated (6-31G*) for the corresponding hydrido bridge between pyridinium ions.[31,32] Experiments and quantum chemical calculations thus indicate significant differences in hydride transfer processes between typical carbocations and pyridinium ions.

Conclusions

Hydride transfer reactions between typical carbocations proceed through tight transition states in which the migrating hydrogen carries a partial positive charge. As a consequence, $\alpha = \delta(\ln k_{ij})/\delta(\ln K_{ij})$ is smaller than 0.5 when the hydride donor is varied and larger than 0.5 when the acceptor is varied. Computational and experimental results indicate the decrease of the intrinsic barriers with decreasing stabilization of the corresponding carbocations and the inappropriateness of α to locate the position of the transition states on the reaction coordinate.

Acknowledgment. This and the preceding paper are dedicated to Professor George A. Olah on the occasion of his 75th

(30) Weinhold, F. *Natural Bond Orbital Methods.* In *Encyclopedia of Computational Chemistry*; Schleyer, P. v. R., Allinger, N. L., Clark, T., Gasteiger, J., Kollman, P. A., Schäfer, H. F., III, Schreiner, P. R., Eds.; Wiley: Chichester, 1998; Vol. 3, pp 1792−1811.
(31) Wu, Y.-D.; Lai, D. K. W.; Houk, K. N. *J. Am. Chem. Soc.* **1995**, *117*, 4100−4108.
(32) Though a general relationship between bond lengths and bond orders has been suggested by Pauling (Pauling, L. *J. Am. Chem. Soc*. **1947**, *69*, 542−553), it has been reported that different parameters have to be employed for different types of bonds: (a) Houk, K. N.; Gustavson, S. M.; Black, K. A. *J. Am. Chem. Soc*. **1992**, *114*, 8565−8572. (b) Zipse, H.; Wang, L.-H.; Houk, K. N. *Liebigs Ann.* **1996**, 1511−1522.

birthday. Financial support by the Deutsche Forschungsgemeinschaft (SFB-424, Münster; Ma 673/18-1, München) and the Fonds der Chemischen Industrie is gratefully acknowledged. We thank Prof. S. Grimme (Münster), Prof. H. Zipse (München), and Prof. M. Kreevoy (Minneapolis) for helpful suggestions, and Prof. D. Aue (Santa Barbara) for his help in selecting appropriate gas-phase data for carbocations.

Supporting Information Available: Kinetic data from ref 16 and details of the calculations (energies of AM1, ab initio, and DFT calculations); Gaussian archive entries (MP2/6-31+G(d,p)//RHF/6-31+G(d,p)) (PDF). This material is available free of charge via the Internet at http://pubs.acs.org.

JA0121540